Published in final edited form as:
Mol Cancer Res. 2012 January ; 10(1): 11–24. doi:10.1158/1541-7786.MCR-11-0256.

Fractalkine Receptor CX3CR1 Is Expressed in Epithelial Ovarian Carcinoma Cells and Required for Motility and Adhesion to Peritoneal Mesothelial Cells

Mijung Kim[1], **Lisa Rooper**[2], **Jia Xie**[1], **Andre A. Kajdacsy-Balla**[2], and **Maria V. Barbolina**[1,*]
[1]Department of Biopharmaceutical Sciences, University of Illinois at Chicago, Chicago, IL 60612
[2]Department of Pathology, University of Illinois at Chicago, Chicago, IL 60612

Abstract

Epithelial ovarian carcinoma is a deadly disease, and little is known about the mechanisms underlying its metastatic progression. Using human specimens and established cell lines, we determined that the G protein-coupled seven-transmembrane fractalkine receptor (CX_3CR1) is expressed in primary and metastatic ovarian carcinoma cells. Ovarian carcinoma cells robustly migrated toward CX_3CL1, a specific ligand of CX_3CR1, in a CX_3CR1-dependent manner. Silencing of CX_3CR1 reduced migration toward human ovarian carcinoma ascites fluid by approximately 70%. Importantly, adhesion of ovarian carcinoma cells to human peritoneal mesothelial cells was dependent on CX_3CL1/CX_3CR1 signaling. In addition, CX_3CL1 was able to induce cellular proliferation. Together, our data suggest that the fractalkine network may function as a major contributor to the progression of epithelial ovarian carcinoma, and further attention to its role in the metastasis of this deadly malignancy is warranted.

Keywords

ovarian carcinoma; CX_3CR1; migration; adhesion; proliferation

INTRODUCTION

Epithelial ovarian carcinoma (EOC) is a relatively rare but highly lethal gynecologic malignancy that claims the lives of over 14,000 women in the US and over 140,000 worldwide (1). EOC is seldomly diagnosed at early stages, when the rate of survival is nearly 90%. Instead, most patients are diagnosed with EOC at late metastatic stages (FIGO stages III – IV) (2). Treatment of advanced and metastatic EOC cases is clinically difficult. The current standard of care includes surgery and chemotherapy with platinum-based drugs (3). However, many EOC cases frequently recur and become insensitive to these therapies (4, 5). Improvement of the existing approaches and development of new therapies to be used either alone or in combination with the existing treatments are necessary to prolong and improve patient survival.

Metastatic EOC spreads throughout the peritoneum largely by sloughing off of the ovary and subsequently attaching to and invading the organs and tissues of the peritoneal cavity. Dissemination through blood and lymphatic vessels, however, is minimal (2, 6). Malignant EOC cells are shed from the ovarian surface and later attach to the mesothelial layer

*Correspondence should be addressed to Maria Barbolina, PhD, University of Illinois at Chicago, 833 S Wood St., PHARM 355, Chicago, IL 60612, USA; phone 7-312-355-0670; mvb@uic.edu.

outlining the peritoneum (2, 7–10). This spreading pattern suggests that the local microenvironment of the peritoneal cavity may contain signals that support homing of the EOC metastasis. Patients with EOC frequently accumulate large volumes (0.5 – 4 L) of peritoneal ascitic fluid. This fluid is a rich source of growth factors, extracellular matrix proteins, chemokines, and other factors that may support and promote peritoneal metastasis (11–13).

The development of new approaches to treat metastatic ovarian carcinoma and the identification of novel pathways for drug targeting could be bolstered by the identification of highly efficacious treatments against molecules involved in metastasis. The goal of this study was to identify methods to prevent or retard metastatic dissemination. Given that identifying new drug target pathways is our priority, we took a focused approach to ascertain the molecules that are most critical for promoting metastasis and can be targeted therapeutically. Chemokine receptors encompass a subclass of G-protein-coupled receptors (GPCRs), which in turn represent a preferred class of drug targets (14). Chemokine receptors show promise for development as therapeutic targets because they have been successfully targeted in the clinic (15) and play a role in homing of metastatic cells to their niches (16–19); however, beyond CXCR4, their role in the development and progression of EOC is largely unknown (11, 20, 21). It is possible that ovarian cancer anti-chemokine receptor antagonists could be useful in preventing metastasis in patients with early stage disease as well as in restricting metastatic spread in patients presenting with advanced stages of malignancy.

We were interested in determining whether chemokine networks that have not yet been implicated in EOC could be important for progression of this malignancy. Preliminary RT-PCR array data in our laboratory suggested that CX_3CR1, a member of the chemokine family of GPCRs, is expressed in cell lines propagated from acute EOC samples. CX_3CR1 is a member of the seven transmembrane CX_3C chemokine receptor group family (22). CX_3CL1, or fractalkine, is the major, highly specific ligand that activates CX_3CR1 (23, 24). This robust ligand specificity suggests that CX_3CR1 could be an attractive target for therapeutic interventions. Interestingly, it has been suggested that CX_3CL1 can also activate another surface receptor, a receptor tyrosine kinase termed epidermal growth factor receptor (EGFR), to stimulate cellular proliferation (25). It has also been reported that poor prognoses and EOC progression correlate with the accumulation of CX_3CR1-positive immunosuppressive leukocytes (26). Because CX_3CR1-positive immunosuppressive leukocytes are attracted to the peritoneal milieu to suppress the native immune system, these findings may suggest that the CX_3CR1-positive EOC cells that are also present in the peritoneum may escape clearance by the native immune system. Escape from immune surveillance and use of immune cell secretions for tumor progression are common features of metastatic tumors (27–31). However, in colon cancer expression of CX_3CL1 correlated with a better prognosis and associated with high densities of T lymphocytes (32).

Here, we show that CX_3CR1 expression is nearly absent in the normal ovarian surface epithelium and that its expression accumulates during the course of tumorigenesis. We also report that CX_3CL1 is present in the ascites of women with EOC or other benign gynecologic conditions. Furthermore, we demonstrate that a functional interaction between CX_3CL1 and CX_3CR1 facilitates cell migration and cell-cell adhesion between EOC cells and peritoneal mesothelial cells. CX_3CL1 is also required for EOC cell proliferation. Because cell migration, proliferation, and peritoneal seeding are crucial for the formation and development of EOC metastasis, our data suggest that fractalkine signaling in EOC may contribute to metastatic dissemination.

MATERIALS AND METHODS

Reagents and Antibodies

Tissue microarray (TMA) slides containing specimens of normal ovary and primary and distant metastatic ovarian carcinoma (Cat# OV208), specimens of normal ovary (Cat# OV806), specimens of serous cystadenoma (Cat# OV603), and specimens of multiple types of ovarian carcinoma (Cat# OV1002) were obtained from US Biomax (Rockville, MD). cDNA arrays prepared from normal ovary and primary ovarian carcinoma specimens were obtained from Origene Technologies (Rockville, MD). CX_3CL1 was obtained from RayBiotech (Norcross, GA). Human collagen type I, type III, bovine serum albumin (BSA), fura-2 AM, and ATP were purchased from Sigma-Aldrich (St. Louis, MO). WST-1 proliferation kits were obtained from Takara Bio (Madison, WI). CX_3CR1 siRNA, control siRNA (#A), a goat anti-human CX_3CR1 antibody (K-13), a rabbit anti-human EGFR antibody, a mouse anti-human GAPDH antibody, a rabbit anti-human PCNA antibody, and total cell lysates from THP-1 and A431 were obtained from Santa Cruz Biotechnology (Santa Cruz, CA). DharmaFECT was obtained from Dharmacon (Lafayette, CO). Matrigel was obtained from BD Biosciences (Bedford, MA). Transwell cell migration chambers with 8 micron pores were purchased from Corning (Corning, NY). AG1478 was obtained from Cayman Chemicals (Ann Arbor, MI). Rabbit polyclonal CX_3CR1 (Cat# ab8020 and ab8021) antibodies and normal rabbit IgG were obtained from Abcam (Cambridge, MA). A FITC-conjugated secondary anti-rabbit IgG was purchased from Invitrogen (Carlsbad, CA). Mouse monoclonal anti-human CX_3CL1 was procured from R&D Systems (Minneapolis, MN), and rabbit anti-human CX_3CL1 was purchased from BioVision (Mountain View, CA). Mouse monoclonal anti-human CD44 and mouse monoclonal anti-β1-integrin (MAB2253) were obtained from Millipore (Billerica, MA). Vectastain ABC and DAB kits were obtained from Vector Laboratories (Burlingame, CA).

Cell Lines

Two human ovarian carcinoma cell lines that originated from malignant cells in the ascites fluid and presented a serous histotype, SKOV-1 and A2780, were obtained from the NCI Tumor Cell Repository (Detrick, MD). These cell lines were cultured as directed by the manufacturer for no longer then twenty consecutive passages. Another human ovarian carcinoma cell line originating from malignant cells in the ascites fluid and presenting a serous histotype, Caov-3, was obtained from Dr. M.S. Stack (University of Missouri-Columbia, MO) and propagated in minimal essential media supplemented by 10% fetal bovine serum (FBS) for no longer than 15 consecutive passages. The human ovarian carcinoma cell line with a serous histotype and originating from a primary tumor, IGROV-1, was obtained from the NCI Tumor Cell Repository (Detrick, MD) and cultured as directed by the manufacturer for no longer than twenty consecutive passages. Two borderline EOC cell lines (HuIOSBT-1.5 and HuIOSBT-3.3) and two normal immortalized human ovarian surface epithelial cell lines (IOSE29 and IOSE80) were obtained from Dr. N. Auersperg through the Canadian Ovarian Tissue Bank (Vancouver, Canada). The normal, immortalized human ovarian surface epithelial cell line HOSE11-12 was obtained from Dr. G.S.W. Tsao (The University of Hong Kong, PRC) and propagated in minimal essential media supplemented with 10% FBS for 5 consecutive passages. The normal immortalized human ovarian surface epithelial cell line T1074 was obtained from Applied Biological Materials (Richmond, Canada) and propagated as directed by the manufacturer. The normal (not immortalized) human ovarian surface epithelial cell line HOSEpiC was purchased from ScienCell Research Laboratories (Carlsbad, CA) and maintained in the conditions suggested by the manufacturer between passages 1 and 2. The human immortalized peritoneal mesothelial cell line LP-9 was obtained from the Coriell Aging Cell Repository (Camden, NJ) and cultured as indicated by the manufacturer for 5–8 passages. All cell lines were

routinely assessed for cellular morphology and average doubling time. All cell lines were propagated from stocks originally obtained from cell banks and individual investigators and have been stored in aliquots for future use. Each aliquot was further propagated for no longer than 20 consecutive passages or 4 months, whichever came first.

Real-Time PCR

Real-time PCR was carried out using the ABI Prizm system (Applied Biosystems) according to the manufacturer's instructions. The following primers were used for detection of CX_3CR1 mRNA in normal ovary and primary EOC samples (obtained from Origene Technologies): CX3CR1FORW 5′CACAAAGGAGCAGGCATGGAAG3′; CX3CR1REV 5′CAGGTTCTCTGTAGACACAAGGC3′. Primers for beta-actin detection (ACTNB) were supplied with the cDNA sample panel (Origene). The iTaq SYBR Green Supermix (Bio-Rad) was used for quantitative PCR as a double-stranded DNA-specific fluorophore. The PCR reaction conditions were as follows: initial denaturation for 10 min at 95 °C followed by 40 cycles of 94°C for 15 sec and 60°C for 30 sec. To determine the specificity of the PCR primers, melting curves were collected by heating the products to 95°C, cooling them to 65°C, and slowly melting them by increasing the temperature 0.5°/sec up to 95 °C. Primers for mRNA detection of our genes of interest were designed using the Primer3 software according to the requirements for real-time RT-PCR oligonucleotide primers.

Immunohistochemistry

TMA slides were deparaffinized by baking at 60°C for 2 h and rehydrated by incubation in xylene, 100% ethanol, 95% ethanol, 70% ethanol, and phosphate buffered saline, pH 7.4, for 5 min each. Peroxidase activity was inhibited with H_2O_2. Antigen retrieval was performed by a 15 min incubation in 1 mM ethylene diamine tetraacetic acid (EDTA; pH 8.0) at 95°C. Prior to primary antibody staining (1:50 dilution (Abcam Cat# ab8021), 1 h at room temperature (RT)) non-specific binding was blocked by incubation with 10% goat serum for 1 h. The biotin-conjugated goat anti-rabbit secondary antibody was used at a 1:200 dilution for 30 min at RT. The Vectashield ABC kit was used as directed by the manufacturer, and tissues were incubated for 45 min at RT. The DAB reagent was prepared as instructed by the manufacturer and applied to tissues on TMA slides for 2 – 10 min until brown color developed. TMAs were stained with hematoxylin, dehydrated in 50%, 70%, 95%, and 100% ethanol, and mounted with Permount. Pancreatic cancer tissue was used as a positive control. Staining was evaluated by A.K.-B. and L.R., who were both blinded to the experimental outcomes of the study. Staining was scored based on the intensity and percentage of positive cells. Intensity of staining was "0" for negative samples, "1" for weakly positive samples, "2" for moderately positive samples, and "3" for highly positive samples. Overall scores were derived as the intensity score multiplied by the percentage. Staining was assessed separately in the cytoplasm and the membrane.

Flow Cytometry

Cells (1×10^6 per tube) were harvested with trypsin/EDTA, resuspended in 100μl of ice cold PBS supplemented with 10% fetal calf serum (FCS) and 1% sodium azide, and fixed in a 1% paraformaldehyde solution in PBS for 15 min on ice. Two micrograms of rabbit anti-human CX_3CR1 antibody (Abcam, ab8021) was added to the cells. For negative controls, the cells were incubated with either 2 μg of anti-rabbit IgG antibody or no primary antibody. Cells were incubated for 1 h on ice in the dark with agitation following washing and resuspension in 400μl ice cold PBS. Two μg of goat anti-rabbit FITC-conjugated IgG (Invitrogen) was added to the cells and incubated for 1 h on ice in the dark with agitation. The cells were washed and resuspended in 400 μl of ice cold PBS supplemented with 2% BSA and 1% sodium azide. Labeled cells were analyzed using a Becton Dickinson LSR I flow cytometer or an Accuri C6 flow cytometer on the same day.

Western Blotting

Western blotting analysis was used to detect the expression of CX_3CR1 and β-tubulin in normal (not immortalized) ovarian surface epithelial cells, normal immortalized ovarian surface epithelial cells, and EOC cell lines. This procedure was performed as previously described (33–35). Antibodies were used at the following dilutions: 1:500 rabbit anti-human-CX_3CR1 (Abcam, ab2080) in a 1×non-animal blocker solution (Vector Laboratories) or 1:200 goat anti-human CX_3CR1 (Santa Cruz Biotechnology, K-13) in 3% BSA in a solution of 50 mM tris-buffered saline, pH 7.4, 150 mM NaCl, and 0.05% Tween-20 (TBST) (Sigma; St. Louis, MO), 1:200 mouse anti-human GAPDH (Santa Cruz Biotechnology) and 1:200 mouse anti-human-β-tubulin (Developmental Studies Hybridoma Bank, Iowa) in 3% BSA in TBST. Immunoreactive bands were visualized with an anti-(rabbit-IgG)-peroxidase, anti-(goat-IgG)-peroxidase, or anti-(mouse-IgG)-peroxidase (Sigma, St. Louis, MO) (1:1000 in 3% BSA in TBST), and enhanced chemiluminescence was read using Chemidoc (Bio-Rad) and Bio-Rad Chemidoc ImageReader software.

Ca^{++} Imaging

Intracellular free calcium concentrations were measured using digital video microfluorimetry as previously described (11). Briefly, SKOV-3 cells were plated on collagen I-coated glass coverslips, rinsed with HEPES buffer, exposed to 10μM fura-2 AM (Molecular Probes, Eugene, OR), and then incubated for 30 min at RT. Complete dye deesterification was achieved by removing the fura-2 AM, rinsing, and maintaining the cells in the dark for 30 min. Glass coverslips were mounted on the stage of a Zeiss AxioObserver inverted epifluorescence microscope equipped for digital fluorescence microscopy. Fluorescence was digitally monitored at 520 nm after excitation at 340 nm (bound Ca^2) and 380 nm (free Ca^{2+}). Ratios of F340/F380 were collected before and during treatment with 20 nM CX_3CL1 using Zeiss software, exported in Excel software and plotted.

Immunofluorescence staining

Cells were cultured on glass coverslips to 50–70% confluence, fixed, permeabilized with 0.01% Triton X-100, and blocked in goat serum. Rabbit anti-human-CX_3CR1 (Abcam, ab8021), rabbit anti-human-CX_3CL1 (BioVision, Mountain View, CA), and rabbit anti-human PCNA (Santa Cruz Biotechnology, Santa Cruz, CA) antibodies were used at a dilution of 1:50. Cells were incubated with the primary antibodies for 1 h at room temperature (22°C). The cells were then incubated with secondary Alexa488-conjugated or Alexa555-conjugated anti-rabbit antibodies (1:500) for 1 h at RT in the dark. 4′,6-Diamidino-2-phenylindole (DAPI) was added to the secondary antibody solution to a final concentration of 10 μg/ml 10 min prior to the end of the incubation period. Cells were washed, air dried, and mounted on glass slides using ProlongGold (Invitrogen, Carlsbad, CA). Fluorescent imaging was performed using a Zeiss AxioObserverD.1 fluorescent microscope.

Transient Transfections

EOC cells were cultured to 80% confluence and transfected with siRNAs using DharmaFECT according to the manufacturer's instructions.

Transwell Cell Migration

Inserts with 0.8 micron porous membranes were bottom-coated with Matrigel (diluted 1:100) for 1 h at 37 °C, rinsed, and dried. Next, 5,000 EOC cells in a final volume of 300 μl were seeded onto the inserts. The inserts were placed in 24-well plates filled with serum-free minimal essential media in the presence or absence of CX_3CL1. Cells were allowed to migrate for 5 h at 37°C and 5% CO_2. Migration was terminated by removing the non-

migrated cells from the inside of the inserts. Cells that did migrate through the membranes were fixed, stained, and counted.

ELISA

Ascites samples from 6 patients with benign (n = 3) or malignant (n = 3) ovarian disease were obtained from ProteoGenex (Culver City, CA) and analyzed for CX_3CL1 using Human CX_3CL1 Quantikine ELISA (R&D Systems, Minneapolis, MN) according to the manufacturer's instructions.

Cell-Cell Adhesion

The human-derived peritoneal mesothelial cell-line LP-9 was cultured in 96-well plates to near confluence. SKOV-3 cells were cultured in monolayers and labeled with fluorescent DiO (Invitrogen) according to the manufacturer's instructions prior to the adhesion assays. They were subsequently released from monolayers with trypsin and resuspended in serum-free cell culture media. When needed, SKOV-3 cells were transiently transfected with either control or CX_3CR1-specific siRNAs and used in adhesion assays between 48 and 72 h from the start of transfection. For the assay, 10,000 DiO-labeled SKOV-3 cells were seeded onto LP-9 monolayers (in sextuplicate for each condition) and allowed to adhere for 5 h at 37 °C and 5% CO_2. Subsequently, the monolayers were washed two times with PBS and fixed in a methanol-containing cell fixative. When required, LP-9 cells were pretreated with CX_3CL1-blocking antibodies for 30 min, and SKOV-3 cells were pretreated with either normal anti-rabbit IgG, anti-CD44, or anti-β1-integrin blocking antibodies for 30 min at 37 °C and 5% CO_2. Adherent cells showing a round cell morphology were visualized by green fluorescent signals using a Zeiss fluorescent microscope. The DiO-labeled cells were then counted, averaged, and characterized as a percentage of adherent cells.

Cell-ECM Adhesion

Tissue culture-treated 48-well plates were pre-coated with 10 μg/ml human collagen type I, 10 μg/ml human collagen type III, Matrigel (diluted 1:100), or 1% BSA for 1 h at 37 °C. The plates were subsequently rinsed with PBS and air dried. Next, 10,000 SKOV-3 cells were seeded (in triplicate for each condition) in coated wells and allowed to adhere for 1 h at 37 °C and 5% CO_2. This seeding was followed by two washes with PBS, fixation in a methanol-containing cell fixative, and staining. Cells were counted, averaged, and plotted.

Cell Proliferation

Cells were seeded in tissue culture-treated 96-well plates and allowed to attach for 6 h following overnight serum starvation (0% serum) at 37°C in 5% CO_2. Cells were plated at a density that yielded confluence below 25% at the beginning of the treatment. Cells were seeded in triplicate for each condition. To assess the proliferative effect of CX_3CL1 on EOC cells, cells were treated with 5 nM, 15 nM, 25 nM CX_3CL1, or 25 nM CX_3CL1 with 5 μM AG1478 for 24 h. Cells treated with complete media containing 10% FBS were used as a positive control. Cells treated with serum-free media served as a negative control. WST-1 was used according to the manufacturer's instructions and incubated with the cells for 1 h following measurement of OD440. A baseline OD440 reading of the mixture of media and WST-1 containing no cells was subtracted from the experimental values.

RESULTS

Expression of CX_3CR1 in Normal and Pathological Ovarian Surface Epithelia

The mechanisms of malignant transformation and metastatic progression of EOC are poorly understood. Current hypotheses have proposed the ovarian surface epithelium and the

fimbriated edge of the fallopian tube as putative cellular origins of the carcinoma (36, 37). It has recently been hypothesized that these two epithelia are part of a transitional epithelium that shares a common origin and is prone to neoplastic transformation due to incomplete differentiation (38). Another unique feature of EOC that is particularly pertinent to the current study is the pattern of metastatic dissemination, which is largely intraperitoneal. The chemokine axis has been associated with homing of malignant cells into their metastatic niches. We hypothesized that the fractalkine axis could play a role in the peritoneal dissemination of EOC. Therefore, we evaluated CX_3CR1 expression in normal and pathological ovarian surface epithelia.

CX_3CR1 expression in normal ovarian surface epithelium was assessed by four methods. Immunohistochemistry was used to detect CX_3CR1 protein expression in normal ovary specimens. CX_3CR1 expression was also measured in normal ovarian surface epithelial cells (HOSEpiC) using immunofluorescence staining, flow cytometry, and Western blot. The majority of the normal epithelial cells (21 cases out of 22) were negative for membranous CX_3CR1 expression (Figure 1A, Supplemental Table 1). Furthermore, 77% of the tested samples (17 out of 22) lacked CX_3CR1 cytoplasmic staining (Supplemental Table 1). Samples were considered negative if the total score was below 100, weakly to moderately positive if the score was between 100 and 200, and strongly positive if the score was above 200. CX_3CR1 expression was not detectable in HOSEpiC cells by immunofluorescence staining, flow cytometry, or Western blot (Figures 1B, 1C, 3A).

Next, we evaluated CX_3CR1 expression in immortalized ovarian surface epithelium. Interestingly, all of the immortalized ovarian surface epithelial cell lines tested (T1074, HOSE11-12, IOSE29, and IOSE80) were CX_3CR1-positive, as demonstrated by flow cytometry and Western blot analysis (Figures 2A, 3A). These findings suggest that induction of CX_3CR1 expression can occur very early in the tumorigenic transformation process.

Subsequently, we evaluated CX_3CR1 expression in specimens of a benign gynecologic condition, ovarian serous cystadenoma, and established cell lines originating from cases with borderline EOC. Flow cytometry also detected positive membranous expression of CX_3CR1 in the borderline EOC cell lines HuIOSBT-1.5 and HuIOSBT-3.3 (Figure 2B). Immunohistochemical analysis of 30 cases of ovarian serous cystadenoma revealed that 83% of the specimens were CX_3CR1-positive in the epithelium (Figure 2C, Supplemental Table 1). A small number of serous cystadenoma cases also showed extensive CX_3CR1 immunoreactivity. Because the clinical prognosis for these cases is excellent, the significance of this finding is unknown.

Furthermore, we utilized RT-PCR and immunohistochemistry to test the RNA and protein expression levels of CX_3CR1 in primary ovarian carcinoma specimens of various histotypes. Our findings revealed that 66 and 50% of the primary EOC cases with a serous histotype were CX_3CR1-positive by RT-PCR (19 out of 29) and immunohistochemistry (12 out of 24), respectively (Supplemental Tables 1 and 2, Figure 3). Among mucinous EOC cases, 3 out of 3 and 13 out of 24 cases were CX_3CR1-positive as demonstrated by RT-PCR and immunohistochemistry, respectively (Supplemental Tables 1 and 2, Figure 3D). RT-PCR analysis identified 5 CX_3CR1-positive cases of endometrioid EOC out of 8 tested (Supplemental Table 2). Notably, nearly all of the cases that received a negative classification by immunohistochemistry did contain some CX_3CR1-positive cells (Supplemental Table 1).

Ovarian carcinoma cell lines derived from primary EOC (IGROV-1) or ascites (Caov-3, SKOV-3, A2780) all showed CX_3CR1 expression, as demonstrated by Western blot, immunofluorescence staining, and flow cytometry (Figure 3). Quantification by ImageJ

software revealed that the intensity of the CX_3CR1 signal in these samples was significantly greater than the background expression observed in pseudopodial protrusions of the SKOV-3 EOC cell line (Figure 3A, graph). SKOV-3 cells responded to the addition of CX_3CL1 by a robust release of intracellular calcium, which is indicative of the ability of CX_3CR1 to support downstream signaling in these cells (Figure 3B).

We tested specimens of metastatic EOC by immunohistochemistry and found that 64% of the specimens (7 out of 11) were CX_3CR1-positive (Figure 3D, Supplemental Table 1). However, nearly all of the samples that were considered negative by immunohistochemistry did contain some CX_3CR1-positive cells (Supplemental Table 2).

Together, our data suggest that CX_3CR1 expression may be induced very early in the course of the tumorigenic transformation of the ovarian surface epithelium.

CX_3CL1 Is Present in the Ascites of Patients with Borderline Gynecologic Diseases and EOC

CX_3CL1 is expressed in many cells and tissues, including the small and large intestine, ovary, and kidney (23, 24, 39, 40). CX_3CL1 exists in either a membrane-inserted form (23, 24) or a soluble form that has been cleaved to facilitate release (41). Peritoneal ascites is a rich source of many compounds, including growth factors, components of the extracellular matrix, and chemokines. Soluble CX_3CL1 is present in the low nanomolar range in the ascites of women with endometriosis (42). We therefore measured CX_3CL1 levels in the ascites of women with EOC and women with borderline gynecologic conditions. By ELISA we found that the average concentration of CX_3CL1 in the ascites from Stage III-IV EOC patients is 2.8 nM. The level is approximately 10-fold lower, 0.18 nM, in the ascites collected from patients with borderline gynecologic diseases (Table 1).

EOC Cells Migrate in a CX_3CL1/CX_3CR1-dependent Manner

Cell migration is essential for metastatic dissemination. Chemokine networks and CX_3CL1/CX_3CR1 in particular have been implicated in the chemotactic migration of tumor cells to distant sites. The presence of soluble CX_3CL1 in the ascites fluid may indicate that this chemokine could serve as an attractive force that guides EOC cells to the peritoneum. Therefore, we tested the ability of CX_3CL1 to attract EOC cells in a Transwell cell migration assay. The addition of 5 nM CX_3CL1 significantly and robustly stimulated the migration of both Caov-3 and SKOV-3 cells by 1.7- and 2.2-fold, respectively (Figure 4A). Silencing of CX_3CR1 with specific siRNAs reduced the ability of SKOV-3 cells to migrate in response to CX_3CL1, to a level that was nearly identical to the control (no CX_3CL1) (Figure 4A). We previously reported a 1.5-fold increase in CXCL12/CXCR4-mediated invasion of EOC cells in the presence of CXCL12 (11). The CXCL12/CXCR4 axis is a well-established driver of metastatic dissemination in EOC (11, 20, 21); in comparison, the CX_3CL1/CX_3CR1 pathway makes an even greater contribution to cell migration.

We next tested the ability of SKOV-3 cells with silenced CX_3CR1 to migrate toward human ascitic fluid obtained from a patient with stage IV EOC (specimen #5, Table 1). Notably, cells with silenced CX_3CR1 displayed a 70% reduction in their ability to migrate compared to control cells expressing CX_3CR1 (Figure 4B). CX_3CR1 siRNA treatment of SKOV-3 cells reduced the total CX_3CR1 expression to 70% (Figure 4B).

CX_3CR1-negative HOSEpiC cells did not display altered migratory ability in the presence of CX_3CL1 (Figure 4C). Interestingly, CX_3CR1-positive T1074 cells did not migrate significantly faster toward CX_3CL1 than controls (Figure 4C). Together, these results demonstrate that CX_3CR1-positive EOC cells show an increased migration ability when

stimulated with CX_3CL1 *in vitro*, whereas immortalized ovarian surface epithelium does not.

EOC Cells Adhere to Human Peritoneal Mesothelial Cells via the CX_3CL1/CX_3CR1 axis

EOC metastatic dissemination occurs largely in the peritoneal cavity. Several molecular interactions, including integrin-ECM, CD44-hyaluronan, CA125-mesothelin, and L1-neuropilin-1, have been shown by both *in vitro* and *in vivo* models to facilitate peritoneal seeding of EOC cells. The CX_3CL1/CX_3CR1 axis has also been shown to promote cell-cell adhesion via the membrane-bound form of CX_3CL1 (22). Thus, we hypothesized that the CX_3CL1/CX_3CR1 interaction could foster EOC-mesothelial adhesion and thereby facilitate metastatic seeding. Prior to confirming this interaction, we determined CX_3CL1 expression in human-derived peritoneal mesothelial LP-9 cells. CX_3CL1 was expressed by the LP-9 cells and present on the cell surface (Figure 5A). Because membrane-anchored CX_3CL1 is present on mesothelial cells, and CX_3CR1 is expressed on EOC cells, this interaction is feasible. To test the role of CX_3CL1/CX_3CR1 in EOC-mesothelial cell adhesion, we performed *in vitro* adhesion assays by co-culturing EOC and mesothelial cells. LP-9 cells were cultured to near complete monolayers. DiO-labeled EOC cells SKOV-3 were seeded on top of the LP-9 monolayers. We found that 90–93% of SKOV-3 cells adhered to the LP-9 monolayer (Figure 5B, images 1 – 2, Supplemental Table 3). Interestingly, siRNA-mediated downregulation of CX_3CR1 resulted in an approximately 50% loss of EOC cell adhesion to the LP-9 cells (Figure 5B, image 3, Supplemental Table 3). Moreover, progressive inhibition of CX_3CL1 by pre-treating LP-9 monolayers with increasing doses of anti-CX_3CL1 antibodies (0.1 μg/ml to 10 μg/ml) prior to the addition of EOC cells resulted in a 50 to 83% decrease in the ability of EOCs to adhere (Figure 5B, images 5 – 7, Supplemental Table 3). Addition of a non-specific IgG did not affect adhesion (Figure 5B, image 4, Supplemental Table 3). In control experiments that tested the consequences of combined inhibition by anti-CD44 and anti-β1-integrin antibodies, the ability of SKOV-3 cells to adhere to LP-9 cells was reduced by 40–50% (Figure 5B, images 8 – 9, Supplemental Table 3). Downregulation of CX_3CR1 or the addition of CX_3CL1 blocking antibodies to CD44- and β1-integrin-blocking antibody treatment further exacerbated the combined effect and resulted in a nearly 70% reduction in SKOV-3-LP-9 adhesion (Figure 5B, panels 10 – 11, Supplemental Table 3).

These data suggest that the CX_3CL1/CX_3CR1 axis plays a significant role in the adhesion of EOC cells to mesothelial cells.

The CX_3CL1/CX_3CR1 Pathway Plays a Small Role in Facilitating EOC Cell Adhesion to Matrigel

After adhesion to mesothelial cells, EOC cells disrupt the cellular monolayer, expose extracellular proteins of the basement membrane, and further invade the submesothelial matrix, which is primarily composed of interstitial collagens type I and III (43). Chemokine networks and the CX_3CL1/CX_3CR1 axis in particular have been shown to promote cell-ECM adhesion (44, 45). Therefore, we hypothesized that this axis could play a role in EOC adhesion to proteins of the submesothelial matrix. To address this question, we tested the ability of SKOV-3 cells to adhere to Matrigel, collagen I, and collagen III. Surprisingly, addition of CX_3CL1 resulted in a slight, but significant, concentration-independent 1.5-fold increase in cell adhesion to Matrigel but not collagens I or III (results not shown). These findings indicate that CX_3CL1/CX_3CR1 plays a small role in promoting ECM adhesion in the initial steps of EOC cell interaction with the proteins of the basement membrane, but it is unlikely to affect adhesion to the deeper layers composed of the collagenous matrix.

CX_3CL1 Is a Potent Inducer of EOC Cell Proliferation

Chemokines are effective inducers of cell proliferation (46). Proliferation plays a prominent role in the virulence of ovarian carcinoma. Metastatic progression of EOC is characterized by a widespread metastasis that far exceeds the size of the primary tumor. Furthermore, the size of the residual tumor after debulking surgery plays a significant role in determining patient survival (47). Our data and previously published results show that high levels of CX_3CL1 are present in the peritoneal milieu in the ascites of patients with various malignant and non-malignant gynecologic diseases (Table 1, (42)). Therefore, we hypothesized that CX_3CL1 could induce the proliferation of EOC cells. We tested CX_3CL1 in a range of concentrations between 5 and 25 nM and found that the majority of immortalized NOSE, borderline, and serous EOC cell lines demonstrated a significant proliferative response to CX_3CL1 stimulation. In several cell lines, including T1074, HuIOSBT-1.5, SKOV-3, and IGROV-1, the addition of CX_3CL1 completely rescued cellular proliferation to a level equal to or higher than the rate of cells stimulated with complete media containing 10% FBS (Figure 6A, B). We also observed a strong induction of nuclear PCNA 24 h after the addition of 25 nM CX_3CL1 to serum-starved SKOV-3 cells (Figure 6B). However, some cell lines, including the immortalized cell line IOSE80 and the borderline EOC cell line HuIOSBT-3.3, demonstrated only slight changes in proliferation in response to CX_3CL1 (Figure 6A). CX_3CL1 can partner with both EGFR and CX_3CR1 to induce cell proliferation (25, 40). Therefore, to assess the contribution of EGFR to CX_3CL1-dependent proliferation, we incubated each of our cell lines with the EGFR inhibitor, AG1478. Interestingly, CX_3CL1-dependent proliferation of all EOC cell lines tested was either inhibited completely or significantly reduced in the presence of AG1478 (Figure 6A). For a more detailed understanding of the role of both CX_3CR1 and EGFR in CX_3CL1-induced proliferation of EOC cells, the receptors were transiently downregulated using specific siRNAs. A proliferation assay revealed that a 70% decrease in CX_3CR1 led to a nearly 50% reduction in CX_3CL1-dependent proliferation. Moreover, an 95% decrease in EGFR resulted in a nearly 90% reduction in CX_3CL1-dependent proliferation (Figure 6C).

Expression of CX3CR1 in Multiple Types of Ovarian Carcinoma

EOC is the most predominant type of ovarian carcinoma. However, ovarian tumors can also arise in stromal cells. Thus, to comprehensively evaluate CX_3CR1 expression in ovarian carcinoma, we evaluated specimens of Krukenberg tumors, yolk sac tumors, dysgerminomas, mature teratomas, Sertoli-stromal cell tumors, granular cell tumors, thecomas, and gynandroblastomas. Our data indicate that the majority of specimens were CX_3CR1-positive (Supplemental Figure 1, Supplemental Table 4). Specifically, 7 out of 10 Krukenberg, 8 out of 8 yolk sac, 8 out of 8 dysgerminoma, 13 out of 13 mature teratomas, 1 out of 1 Sertoli-stromal cell, 13 out of 15 granular cell, 14 out of 14 thecomas, and 1 out of 1 gynandroblastoma tumor specimens were CX_3CR1-positive, suggesting that fractalkine signaling may affect the progression of all of these tumors. Importantly, these data demonstrate that cancers beyond those of epithelial origin may depend on fractalkine signaling.

DISCUSSION

The mechanisms underlying peritoneal dissemination of ovarian carcinoma are poorly understood. Ovarian carcinoma is a malignancy with an exceptionally high mortality rate (1), largely due to the lack of effective anti-metastatic treatment approaches. A more detailed understanding of the mechanisms underlying the formation and development of EOC metastases could offer insights into how late stages of this disease might be effectively targeted. Proteins that are presented on the cell surface have consistently been considered attractive molecular targets for disease treatment. Our data suggest that a member of GPCR

family, the chemokine fractalkine receptor, functions to support the pro-metastatic properties of EOC cells, which include migration, peritoneal adhesion, and proliferation. In addition, the fractalkine chemokine can support cell proliferation through another receptor, EGFR. Our data support the hypothesis that multiple types of ovarian carcinoma rely on fractalkine signaling for disease progression.

Peritoneal metastasis is a terminal stage of EOC progression. Nevertheless, the mechanistic details of mesothelial adhesion are poorly understood. Several molecular interactions between EOC cells and CD44, β1-integrin, L1, and CA125 as well as between mesothelial cells and hyaluronan, fibronectin, neuropilin-1, and mesothelin have been shown to contribute to peritoneal attachment both *in vitro* and *in vivo* (8, 48–51). Despite these findings, which demonstrate the importance of mesothelial adhesion, a complete understanding of all factors that play a role in EOC cell adhesion to the peritoneum has yet to be presented. Moreover, it is expected that differences in patient-specific expression levels and isoform heterogeneity of peritoneal adhesion-stimulating molecules (7, 52, 53) will diminish the extensive inhibition observed in both cell culture and xenograft models. Thus, it is imperative to elucidate other factors that contribute to mesothelial adhesion, which is a key initial step in the metastatic colonization of the peritoneal cavity. To this end, our data strongly suggest that the fractalkine network originating between CX_3CR1-positive EOC cells and CX_3CL1-positive mesothelial cells could play a role in cell-cell adhesion. There may be several potential mechanisms whereby this interaction bridges cell-cell attachment. A traditional mechanism utilized by rolling leukocytes involves interaction of surface-expressed chemokine receptors with chemokines presented on the glycosaminoglycans chains of endothelial cells following integrin activation (22, 54). CX_3CL1, however, is a transmembrane protein, and it has been previously shown that CX_3CL1-mediated cell-cell adhesion can take place in the absence of integrin activation (22, 54). Our data support the latter mechanism as we have observed an additive negative effect on cell adhesion from simultaneous disruption of CX_3CL1/CX_3CR1-, β1-integrin-, and CD44-dependent modes of adhesion.

Our data indicate that two additional properties of the metastatic cell, migration and proliferation, are dependent on fractalkine signaling as well. We show that the CX_3CL1/CX_3CR1 pair plays a pivotal role in facilitating cell motility. This property may have implications for all stages of EOC metastatic progression. CX_3CL1 is present in the ascites fluid of EOC patients at levels that allow for productive CX_3CL1/CX_3CR1 signaling, which might induce shedding of the malignant cells and locoregional migration of the cells comprising growing metastatic lesions. Interestingly, our data, albeit limited by the number of specimens, indicate that the level of CX_3CL1 in the ascites fluid of patients with benign gynecologic diseases is an order of magnitude lower than that of the EOC ascites. These data suggest that although CX_3CR1 is expressed in transformed cells, CX_3CL1-mediated migration off of the ovarian surface is unlikely to occur due to the lower than optimal levels of the ligand, as the IC50 and Kd of CX_3CL1 and CX_3CR1 binding were estimated at 2.4 and 1.7 nM, respectively (55, 56). Thus, the benign tumors might harbor the potential for future activation of CX_3CL1/CX_3CR1-dependent migration.

The present work also reveals a role for fractalkine signaling in EOC cell proliferation. Our data suggest that both EGFR and CX_3CR1 could be the primary receptors supporting CX_3CL1-dependent EOC cell proliferation. Proliferation plays a significant role in the progression of peritoneal metastasis from EOC. EOC is characterized by a vast uncontrolled spread of metastasis through the peritoneum. Moreover, because an estimated 48% of EOC cases are EGFR-positive (57), and our studies demonstrate that the majority of EOC cases are CX_3CR1-positive, CX_3CL1 could be considered an important contributor to EOC cell proliferation.

Taken together, our data indicate that both fractalkine and its receptor may facilitate the metastatic progression of EOC by participating in migration, proliferation, and peritoneal adhesion. Hence, both fractalkine and its receptor may become useful therapeutic targets. Targeted inhibition of both membrane-bound and soluble CX_3CL1, as well as its receptor CX_3CR1, could result in impaired migration, adhesion, and proliferation. However, additional studies are required to validate our *in vitro* data and disclose the impact of these pathways (CX_3CL1/EGFR and CX_3CL1/CX_3CR1) on the development of metastasis *in vivo*. Interestingly, a possibility of the "cross-talk" between CXCL12/CXCR4 and EGFR, which may result in linking signals of cell proliferation in ovarian carcinoma, has been suggested before (58). Thus, it is interesting to speculate that activated CX_3CR1, which belongs to the family of chemokine receptors along with CXCR4, may activate EGFR-dependent proliferation using a similar "cross-talk" mechanism.

It has been proposed that the CX_3CL1/CX_3CR1 pathway could become a major therapeutic target due to its involvement in various pathologic conditions, such as inflammation, pain, and cancer (59). Although no anti-CX_3CL1 or anti-CX_3CR1 therapies are currently available, a few studies have demonstrated the efficacy of several compounds in preclinical studies. For example, an analog of CX_3CL1 that has an inhibitory effect on CX_3CR1 during inflammation was recently discovered (60). A small molecule inhibitor of CX_3CR1, AZ12201182, was effective in abrogating mitosis and apoptosis (25). In another report, nicotinic acid was shown to effectively suppress fractalkine and other chemokines in adipocytes (61). Although there are cases in which various diseases were successfully alleviated by targeting chemokine receptors, challenges in drug design and efficacy, the existence of multiple receptors driving the disease, species differences and relevance of the target to the human disease, among others, have also been reported (62). Thus, the clinical efficacy of future CX_3CR1-targeting agents remains to be confirmed.

Supplementary Material

Refer to Web version on PubMed Central for supplementary material.

Acknowledgments

We thank Dr. Penzes for the critical reading of the manuscript. This work was supported by the National Institutes of Health grant 1R21CA160917 (to M.V.B.).

References

1. Jemal A, Siegel R, Xu J, Ward E. Cancer statistics. CA Cancer J Clin. 2010; 60:277–300. [PubMed: 20610543]
2. Cannistra SA. Cancer of the ovary. N Engl J Med. 2004; 351:2519–29. [PubMed: 15590954]
3. Armstrong DK, Bundy B, Wenzel L, et al. Intraperitoneal cisplatin and paclitaxel in ovarian cancer. N Engl J Med. 2006; 354:34–43. [PubMed: 16394300]
4. Martin LP, Schilder RJ. Management of recurrent ovarian carcinoma: current status and future directions. Semin Oncol. 2009; 36:112–25. [PubMed: 19332246]
5. Vasey PA. Management of recurrent epithelial ovarian carcinoma. Aust N Z J Obstet Gynaecol. 2005; 45:269–77. [PubMed: 16029291]
6. Lengyel E. Ovarian cancer development and metastasis. Am J Pathol. 2010; 177:1053–64. [PubMed: 20651229]
7. Cannistra SA, DeFranzo B, Niloff J, Ottensmeir C. Functional heterogeneity of CD44 molecules in ovarian cancer cell lines. Clin Cancer Res. 1995; 1:333–42. [PubMed: 9815989]
8. Cannistra SA, Kansas GS, Niloff J, DeFranzo B, Kim Y, Ottensmeier C. Binding of ovarian cancer cells to peritoneal mesothelium in vitro is partly mediated by CD44H. Cancer Res. 1993; 53:3830–8. [PubMed: 8339295]

9. Casey RC, Skubitz AP. CD44 and beta1 integrins mediate ovarian carcinoma cell migration toward extracellular matrix proteins. Clinical & Experimental Metastasis. 2000; 18:67–75. [PubMed: 11206841]
10. Khan SM, Funk HM, Thiolloy S, et al. In vitro metastatic colonization of human ovarian cancer cells to the omentum. Clin Exp Metastasis. 27:185–96. [PubMed: 20229256]
11. Barbolina MV, Kim M, Liu Y, et al. Microenvironmental regulation of chemokine (C-X-C-motif) receptor 4 in ovarian carcinoma. Mol Cancer Res. 8:653–64. [PubMed: 20460402]
12. Kohn EC, Travers LA, Kassis J, Broome U, Klominek J. Malignant effusions are sources of fibronectin and other promigratory and proinvasive components. Diagn Cytopathol. 2005; 33:300–8. [PubMed: 16240400]
13. Sood A, Moudgil A, Sood N, Kharay AS, Kaushal S, Narang AP. Role of fibronectin in diagnosis of malignant ascites. J Assoc Physicians India. 1997; 45:283–5. [PubMed: 12521085]
14. Williams C, Hill SJ. GPCR signaling: understanding the pathway to successful drug discovery. Methods Mol Biol. 2009; 552:39–50. [PubMed: 19513640]
15. Viola A, Luster AD. Chemokines and their receptors: drug targets in immunity and inflammation. Annu Rev Pharmacol Toxicol. 2008; 48:171–97. [PubMed: 17883327]
16. Balkwill F. Cancer and the chemokine network. Nat Rev Cancer. 2004; 4:540–50. [PubMed: 15229479]
17. Jamieson WL, Shimizu S, D'Ambrosio JA, Meucci O, Fatatis A. CX3CR1 is expressed by prostate epithelial cells and androgens regulate the levels of CX3CL1/fractalkine in the bone marrow: potential role in prostate cancer bone tropism. Cancer Res. 2008; 68:1715–22. [PubMed: 18339851]
18. Marchesi F, Piemonti L, Fedele G, et al. The chemokine receptor CX3CR1 is involved in the neural tropism and malignant behavior of pancreatic ductal adenocarcinoma. Cancer Res. 2008; 68:9060–9. [PubMed: 18974152]
19. Shulby SA, Dolloff NG, Stearns ME, Meucci O, Fatatis A. CX3CR1-fractalkine expression regulates cellular mechanisms involved in adhesion, migration, and survival of human prostate cancer cells. Cancer Res. 2004; 64:4693–8. [PubMed: 15256432]
20. Kajiyama H, Shibata K, Terauchi M, Ino K, Nawa A, Kikkawa F. Involvement of SDF-1alpha/CXCR4 axis in the enhanced peritoneal metastasis of epithelial ovarian carcinoma. International Journal of Cancer. 2008; 122:91–9.
21. Scotton CJ, Wilson JL, Scott K, et al. Multiple actions of the chemokine CXCL12 on epithelial tumor cells in human ovarian cancer. Cancer Research. 2002; 62:5930–8. [PubMed: 12384559]
22. Imai T, Hieshima K, Haskell C, et al. Identification and molecular characterization of fractalkine receptor CX3CR1, which mediates both leukocyte migration and adhesion. Cell. 1997; 91:521–30. [PubMed: 9390561]
23. Bazan JF, Bacon KB, Hardiman G, et al. A new class of membrane-bound chemokine with a CX3C motif. Nature. 1997; 385:640–4. [PubMed: 9024663]
24. Pan Y, Lloyd C, Zhou H, et al. Neurotactin, a membrane-anchored chemokine upregulated in brain inflammation. Nature. 1997; 387:611–7. [PubMed: 9177350]
25. White GE, Tan TC, John AE, Whatling C, McPheat WL, Greaves DR. Fractalkine has anti-apoptotic and proliferative effects on human vascular smooth muscle cells via epidermal growth factor receptor signalling. Cardiovasc Res. 85:825–35. [PubMed: 19840952]
26. Hart KM, Bak SP, Alonso A, Berwin B. Phenotypic and functional delineation of murine CX(3)CR1 monocyte-derived cells in ovarian cancer. Neoplasia. 2009; 11:564–73. 1 p following 73. [PubMed: 19484145]
27. Lin A, Schildknecht A, Nguyen LT, Ohashi PS. Dendritic cells integrate signals from the tumor microenvironment to modulate immunity and tumor growth. Immunol Lett. 127:77–84. [PubMed: 19778555]
28. Nelson DS, Nelson M. Evasion of host defences by tumours. Immunol Cell Biol. 1987; 65 (Pt 4): 287–304. [PubMed: 3315983]
29. Ohm JE, Carbone DP. Immune dysfunction in cancer patients. Oncology (Williston Park). 2002; 16:11–8. [PubMed: 11829278]

30. Takaishi K, Komohara Y, Tashiro H, et al. Involvement of M2-polarized macrophages in the ascites from advanced epithelial ovarian carcinoma in tumor progression via Stat3 activation. Cancer Sci. 101:2128–36. [PubMed: 20860602]
31. Labidi-Galy SI, Sisirak V, Meeus P, et al. Quantitative and functional alterations of plasmacytoid dendritic cells contribute to immune tolerance in ovarian cancer. Cancer Res. 71:5423–34. [PubMed: 21697280]
32. Mlecnik B, Tosolini M, Charoentong P, et al. Biomolecular network reconstruction identifies T-cell homing factors associated with survival in colorectal cancer. 138:1429–40.
33. Barbolina M, Adley BP, Kelly DL, Fought AJ, Scholtens DM, Shea LD, Stack MS. Motility-related actinin alpha-4 is associated with advanced and metastatic ovarian carcinoma. Lab Invest. 2008; 88:602–14. [PubMed: 18362906]
34. Barbolina MV, Adley BP, Ariztia EV, Liu Y, Stack MS. Microenvironmental Regulation of Membrane Type 1 Matrix Metalloproteinase Activity in Ovarian Carcinoma Cells via Collagen-induced EGR1 Expression. J Biol Chem. 2007; 282:4924–31. [PubMed: 17158885]
35. Barbolina MV, Adley BP, Shea LD, Stack MS. Wilms tumor gene protein 1 is associated with ovarian cancer metastasis and modulates cell invasion. Cancer. 2008; 112:1632–41. [PubMed: 18260155]
36. Levanon K, Crum C, Drapkin R. New insights into the pathogenesis of serous ovarian cancer and its clinical impact. J Clin Oncol. 2008; 26:5284–93. [PubMed: 18854563]
37. Pothuri B, Leitao MM, Levine DA, et al. Genetic analysis of the early natural history of epithelial ovarian carcinoma. PLoS One. 5:e10358. [PubMed: 20436685]
38. Auersperg N. The origin of ovarian carcinomas: a unifying hypothesis. Int J Gynecol Pathol. 30:12–21. [PubMed: 21131839]
39. Lucas AD, Chadwick N, Warren BF, et al. The transmembrane form of the CX3CL1 chemokine fractalkine is expressed predominantly by epithelial cells in vivo. Am J Pathol. 2001; 158:855–66. [PubMed: 11238035]
40. Gaudin F, Nasreddine S, Donnadieu AC, et al. Identification of the chemokine CX3CL1 as a new regulator of malignant cell proliferation in epithelial ovarian cancer. PloS one. 6:e21546. [PubMed: 21750716]
41. Garton KJ, Gough PJ, Blobel CP, et al. Tumor necrosis factor-alpha-converting enzyme (ADAM17) mediates the cleavage and shedding of fractalkine (CX3CL1). J Biol Chem. 2001; 276:37993–8001. [PubMed: 11495925]
42. Shimoya K, Zhang Q, Temma-Asano K, Hayashi S, Kimura T, Murata Y. Fractalkine in the peritoneal fluid of women with endometriosis. Int J Gynaecol Obstet. 2005; 91:36–41. [PubMed: 16109418]
43. Harvey W, Amlot PL. Collagen production by human mesothelial cells in vitro. Journal of Pathology. 1983; 139:337–47. [PubMed: 6834177]
44. Goda S, Imai T, Yoshie O, et al. CX3C-chemokine, fractalkine-enhanced adhesion of THP-1 cells to endothelial cells through integrin-dependent and -independent mechanisms. J Immunol. 2000; 164:4313–20. [PubMed: 10754331]
45. Lloyd AR, Oppenheim JJ, Kelvin DJ, Taub DD. Chemokines regulate T cell adherence to recombinant adhesion molecules and extracellular matrix proteins. J Immunol. 1996; 156:932–8. [PubMed: 8558019]
46. Wang JM, Deng X, Gong W, Su S. Chemokines and their role in tumor growth and metastasis. J Immunol Methods. 1998; 220:1–17. [PubMed: 9839921]
47. Chi DS, Eisenhauer EL, Zivanovic O, et al. Improved progression-free and overall survival in advanced ovarian cancer as a result of a change in surgical paradigm. Gynecol Oncol. 2009; 114:26–31. [PubMed: 19395008]
48. Arlt MJ, Novak-Hofer I, Gast D, et al. Efficient inhibition of intra-peritoneal tumor growth and dissemination of human ovarian carcinoma cells in nude mice by anti-L1-cell adhesion molecule monoclonal antibody treatment. Cancer Res. 2006; 66:936–43. [PubMed: 16424028]
49. Sawada K, Mitra AK, Radjabi AR, et al. Loss of E-cadherin promotes ovarian cancer metastasis via alpha 5-integrin, which is a therapeutic target. Cancer Res. 2008; 68:2329–39. [PubMed: 18381440]

50. Scholler N, Garvik B, Hayden-Ledbetter M, Kline T, Urban N. Development of a CA125-mesothelin cell adhesion assay as a screening tool for biologics discovery. Cancer Lett. 2007; 247:130–6. [PubMed: 16677756]
51. Strobel T, Cannistra SA. Beta1-integrins partly mediate binding of ovarian cancer cells to peritoneal mesothelium in vitro. Gynecol Oncol. 1999; 73:362–7. [PubMed: 10366461]
52. Daponte A, Kostopoulou E, Kollia P, et al. L1 (CAM) (CD171) in ovarian serous neoplasms. Eur J Gynaecol Oncol. 2008; 29:26–30. [PubMed: 18386459]
53. Bast RC Jr, Klug TL, St John E, et al. A radioimmunoassay using a monoclonal antibody to monitor the course of epithelial ovarian cancer. N Engl J Med. 1983; 309:883–7. [PubMed: 6310399]
54. Fong AM, Robinson LA, Steeber DA, et al. Fractalkine and CX3CR1 mediate a novel mechanism of leukocyte capture, firm adhesion, and activation under physiologic flow. J Exp Med. 1998; 188:1413–9. [PubMed: 9782118]
55. Davis CN, Zujovic V, Harrison JK. Viral macrophage inflammatory protein-II and fractalkine (CX3CL1) chimeras identify molecular determinants of affinity, efficacy, and selectivity at CX3CR1. Mol Pharmacol. 2004; 66:1431–9. [PubMed: 15361546]
56. Nakayama T, Watanabe Y, Oiso N, et al. Eotaxin-3/CC chemokine ligand 26 is a functional ligand for CX3CR1. JImmunol. 185:6472–9. [PubMed: 20974991]
57. Lafky JM, Wilken JA, Baron AT, Maihle NJ. Clinical implications of the ErbB/epidermal growth factor (EGF) receptor family and its ligands in ovarian cancer. Biochim Biophys Acta. 2008; 1785:232–65. [PubMed: 18291115]
58. Porcile C, Bajetto A, Barbieri F, et al. Stromal cell-derived factor-1alpha (SDF-1alpha/CXCL12) stimulates ovarian cancer cell growth through the EGF receptor transactivation. Exp Cell Res. 2005; 308:241–53. [PubMed: 15921680]
59. D'Haese JG, Demir IE, Friess H, Ceyhan GO. Fractalkine/CX3CR1: why a single chemokine-receptor duo bears a major and unique therapeutic potential. Expert Opin Ther Targets. 14:207–19. [PubMed: 20055718]
60. Dorgham K, Ghadiri A, Hermand P, et al. An engineered CX3CR1 antagonist endowed with anti-inflammatory activity. J Leukoc Biol. 2009; 86:903–11. [PubMed: 19571253]
61. Digby JE, McNeill E, Dyar OJ, Lam V, Greaves DR, Choudhury RP. Anti-inflammatory effects of nicotinic acid in adipocytes demonstrated by suppression of fractalkine, RANTES, and MCP-1 and upregulation of adiponectin. Atherosclerosis. 209:89–95. [PubMed: 19781706]
62. Horuk R. Chemokine receptor antagonists: overcoming developmental hurdles. Nat Rev Drug Discov. 2009; 8:23–33. [PubMed: 19079127]

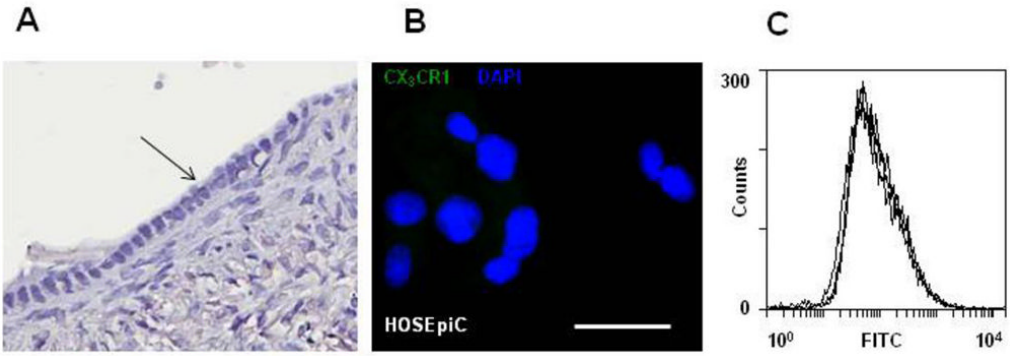

Figure 1. CX_3CR1 is not expressed in normal ovarian surface epithelium

(A) Samples from normal ovaries were examined for CX_3CR1 expression by immunohistochemistry. The black arrow indicates the ovarian surface epithelium. Brown – CX_3CR1; blue – hematoxylin. Images were generated using an Aperio ScanScope digital slide scanner. Magnification – 20×. (B) Expression of CX_3CR1 in normal ovarian surface epithelial cells (HOSEpiC) was evaluated by immunofluorescent staining. CX_3CR1 – green; DAPI – blue. Images were collected on the green and blue filters independently and then superimposed. Bar, 50μm. (C) Cell surface expression of CX_3CR1 in HOSEpiC was analyzed by flow cytometry. CX_3CR1 expression in HOSEpiC and negative controls (normal rabbit IgG plus FITC-conjugated goat anti-rabbit IgG and FITC-conjugated goat anti-rabbit IgG only) is shown. The results are representative of three independent experiments.

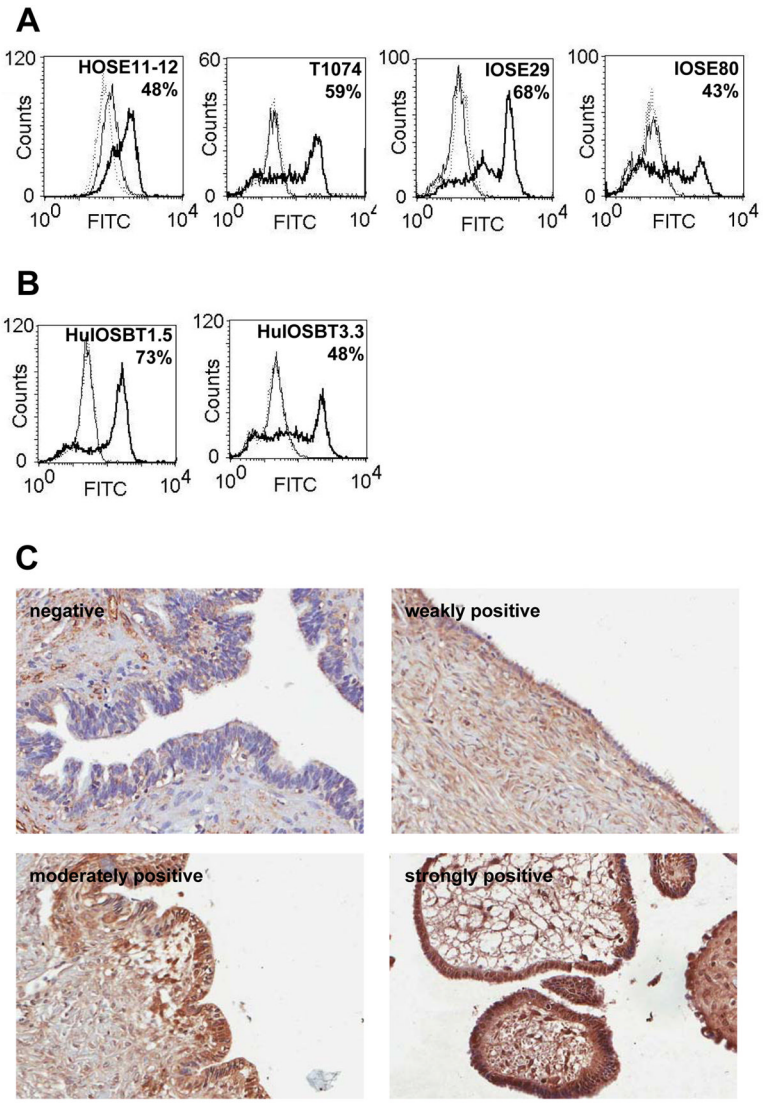

Figure 2. CX_3CR1 is expressed in immortalized and borderline EOC cell lines as well as human serous cystadenoma specimens

Cell surface expression of CX_3CR1 in immortalized NOSE (A) and borderline EOC cells lines (B) was analyzed by flow cytometry. The percentage of positive cells is indicated. Solid thick line – CX_3CR1 expression; solid thin line – negative control (normal rabbit IgG and FITC-conjugated goat anti-rabbit IgG); dotted line – negative control (FITC-conjugated goat anti-rabbit IgG only). These data are representative of at least three independent experiments. (C) Expression of CX_3CR1 in cases of benign serous cystadenoma was determined by immunohistochemistry. Brown – CX_3CR1; blue – hematoxylin. Images were generated using an Aperio ScanScope digital slide scanner. Magnification – 10×. Examples of CX_3CR1-negative (core C7, Supplemental Table 3), weakly positive (core B4, Supplemental Table 3), moderately positive (core D2, Supplemental Table 3), and strongly positive (core E3, Supplemental Table 3) specimens are presented.

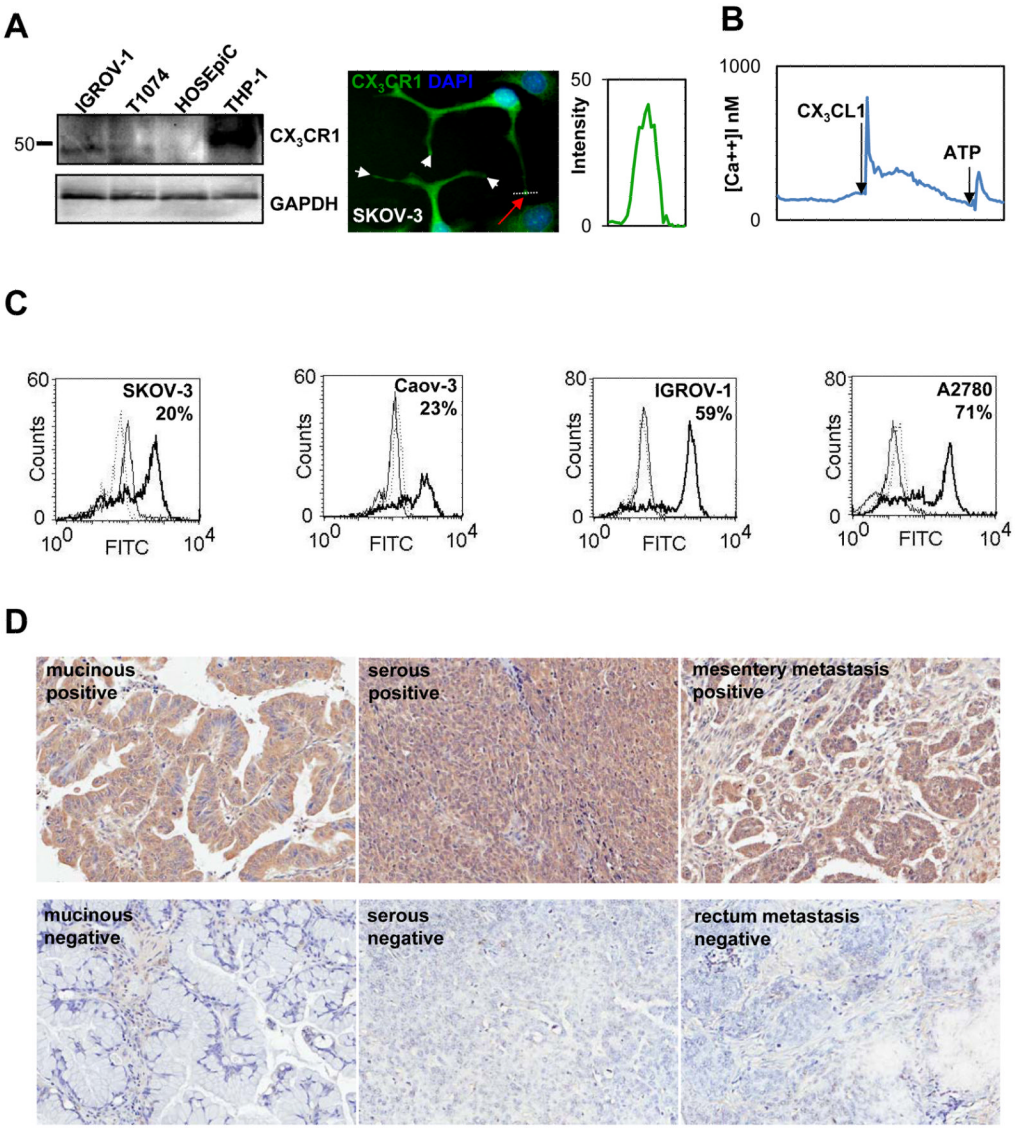

Figure 3. CX_3CR1 is expressed in primary and metastatic epithelial ovarian carcinoma

(A) CX_3CR1 expression in normal ovarian surface epithelial cells (HOSEpiC), immortalized normal ovarian surface epithelial cells (T1074), and serous EOC cell line (IGROV-1) was evaluated by Western blot. GAPDH served as a loading control. THP-1 cell lysate was used as a positive control for CX_3CR1 expression. Position of the marker lane of apparent molecular weight of 50 kDa is indicated. Expression of CX_3CR1 in the serous EOC cell line (SKOV-3) was evaluated using immunofluorescence staining. CX_3CR1 – green; DAPI – blue. Images were collected independently on the green and blue filters and subsequently superimposed. Bar, 10 μm. Histogram shows the intensity of CX_3CR1 staining across the pseudopodial protrusions of SKOV-3 cells (white dotted line and red arrow). (B) Intracellular $[Ca^{++}]$ changes in response to 20 nM CX_3CL1 indicate the presence of active CX_3CR1 in EOC cells. An ATP-induced signal indicates live cells. (C) Cell surface expression of CX_3CR1 in the indicated serous EOC cell lines was analyzed by flow cytometry. The percentage of positive cells is indicated. Solid thick line – CX_3CR1 expression; solid thin line – negative control (normal rabbit IgG and FITC-conjugated goat anti-rabbit IgG); dotted line – negative control (FITC-conjugated goat anti-rabbit IgG only).

These data are representative of at least three independent experiments. (D) Expression of CX_3CR1 in cases of primary and metastatic EOC was determined by immunohistochemistry. Brown – CX_3CR1; blue – hematoxylin. Images were generated using an Aperio ScanScope digital slide scanner. Magnification - 10×. Examples of CX_3CR1-positive and CX_3CR1-negative cases of mucinous adenocarcinoma (cores C10 and C5, respectively, Supplemental Table 1), serous carcinoma (cores I15 and G9, respectively, Supplemental Table 1), and metastatic serous carcinoma (cores J8 and L3, respectively, Supplemental Table 1) are displayed.

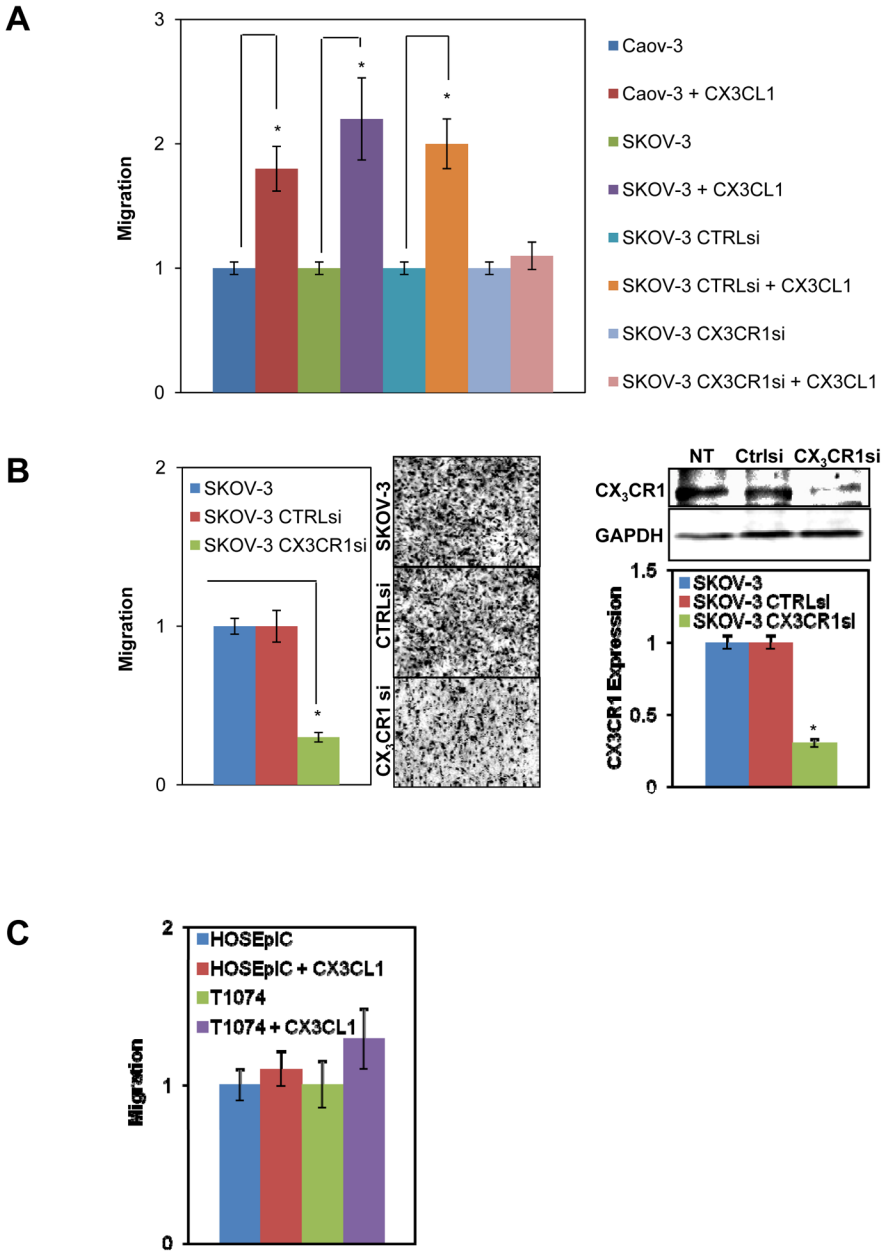

Figure 4. CX_3CL1/CX_3CR1-dependent cell migration

(A) Two EOC cell lines, Caov-3 and SKOV-3, were either not transfected, transfected with control siRNA, or transfected with CX_3CR1 siRNA and then subjected to a cell migration assay in a Transwell chamber in the presence or absence of 5 nM CX_3CL1 for 5 h. (B) SKOV-3 cells were either not transfected or transiently transfected with control or CX_3CR1 siRNAs and then subjected to a Transwell cell migration assay using human peritoneal ascites fluid (specimen #5, respectively, Table 2). Images on the right illustrate the numbers of migrated cells in each condition. Downregulation of CX3CR1 by siRNA in SKOV-3 cells was analyzed by Western blot and quantified by digital densitometry. GAPDH served as a loading control. *p<0.05. (C) Normal ovarian surface epithelial cells (HOSEpiC) and immortalized ovarian surface epithelial cells (T1074) were allowed to migrate for 5 h in the presence or absence of 5 nM CX_3CL1 in a Transwell chamber. The number of cells that

migrated in the control condition without added CX_3CL1 was set as “1”, and other values were calculated relative to this level. These data represent the average of three experiments performed in triplicate. *p<0.05.

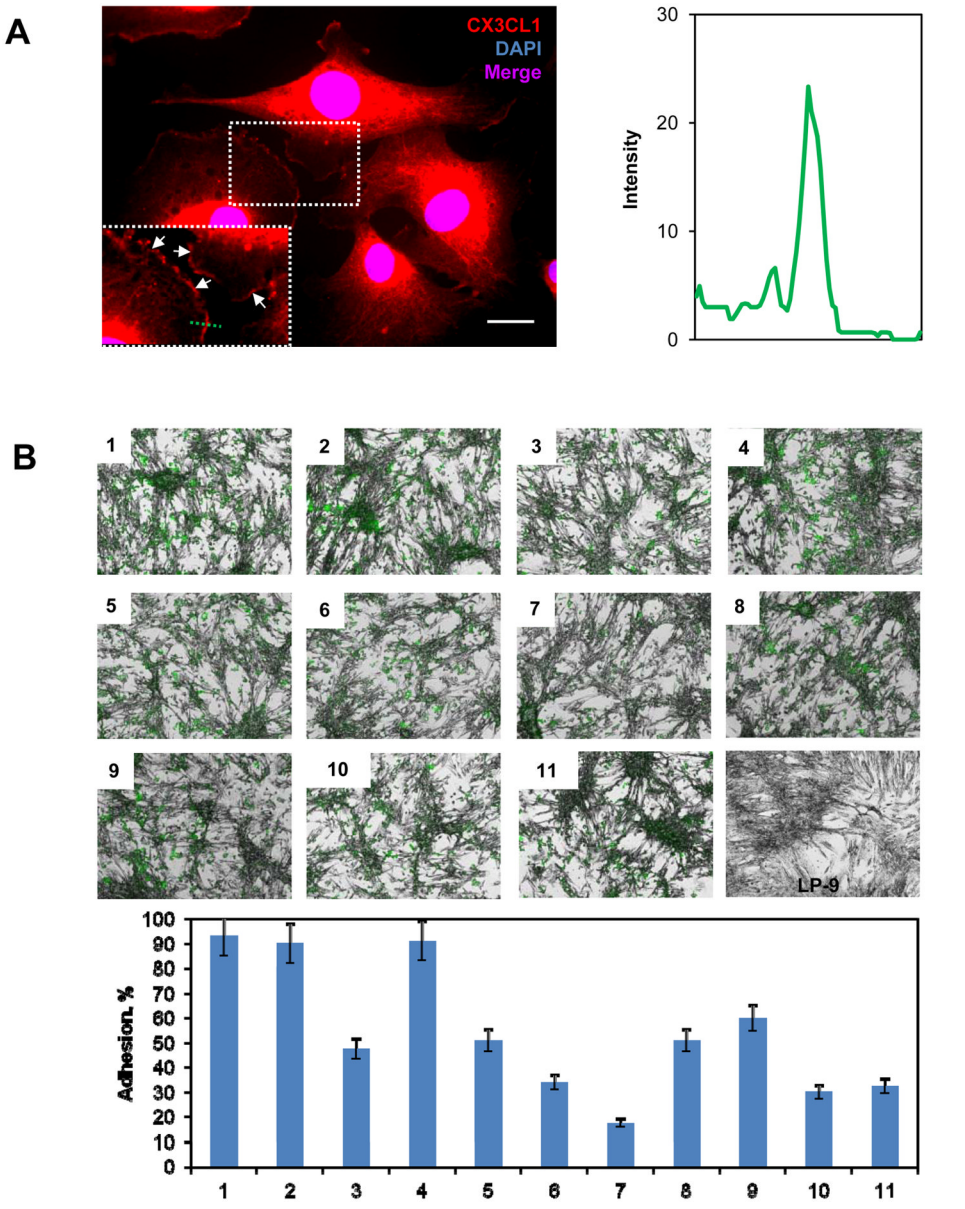

Figure 5. EOC cells adhere to peritoneal mesothelial cells and Matrigel in a CX_3CL1/CX_3CR1-dependent manner

(A) Immunofluorescence analysis of CX_3CL1 expression in LP-9 cells. The rabbit anti-human CX_3CL1 antibody (BioVision) was used at a dilution of 1:50, and the goat anti-rabbit AlexaFluor546 antibody (Molecular Probes) was used at a dilution of 1:500. Nuclei were counterstained with DAPI. CX_3CL1 – red; DAPI – blue. Images were collected independently with red and blue filters and subsequently superimposed. Bar, 5 μm. The insert shows a 1.5-fold enlarged rectangular area outlined by dotted lines. White arrows indicate membranous CX_3CL1 staining. The histogram shows the intensity of CX_3CL1 staining across the membrane of an LP-9 cell (along the green dotted line). (B) SKOV-3 cell adhesion to LP-9 monolayers is shown. LP-9 cells were cultured in monolayers. SKOV-3 cells were labeled with DiO, a fluorescent tracking dye, prior to the adhesion assays. Adhesion assays were performed over 5 h. Adhered cells were fixed with 4% paraformaldehyde, and images were taken using green fluorescence and bright field

microscopy with a 5× magnification objective and a Zeiss fluorescent microscope. The images were then superimposed. Green – SKOV-3; grey – LP-9. The following conditions were evaluated: 1) SKOV3 adhesion to LP-9 cells; 2) control siRNA-transfected SKOV-3 cell adhesion to LP-9 cells; 3) CX_3CR1 siRNA-transfected cell adhesion to LP-9 cells; 4) SKOV-3 cell adhesion to LP-9 cells pre-treated with IgG; 5) SKOV-3 cell adhesion to LP-9 cells pre-treated with 0.1 μg/ml CX_3CL1 blocking antibodies; 6) SKOV-3 cell adhesion to LP-9 cells pre-treated with 1 μg/ml CX_3CL1 blocking antibodies; 7) SKOV-3 cell adhesion to LP-9 cells pre-treated with 10 μg/ml CX_3CL1 blocking antibodies; 8) SKOV-3 cell adhesion to LP-9 cells pre-treated with 1 μg/ml CD44 blocking antibodies and 1 μg/ml β1-integrin blocking antibodies; 9) control siRNA-transfected SKOV-3 cell adhesion to LP-9 cells pre-treated with 1 μg/ml CD44 blocking antibodies and 1 μg/ml β1-integrin blocking antibodies; 10) CX_3CR1 siRNA-transfected SKOV-3 cell adhesion to LP-9 cells pre-treated with 1 μg/ml CD44 blocking antibodies and 1 μg/ml β1-integrin blocking antibodies; 9) SKOV-3 cell adhesion to LP-9 cells pre-treated with 1 μg/ml CX_3CL1 blocking antibodies, 1 μg/ml CD44 blocking antibodies, and 1 μg/ml β1-integrin blocking antibodies. These data represent the average of three experiments performed in sextuplicate. A quantitative analysis of the adhesion data is presented in the histogram.

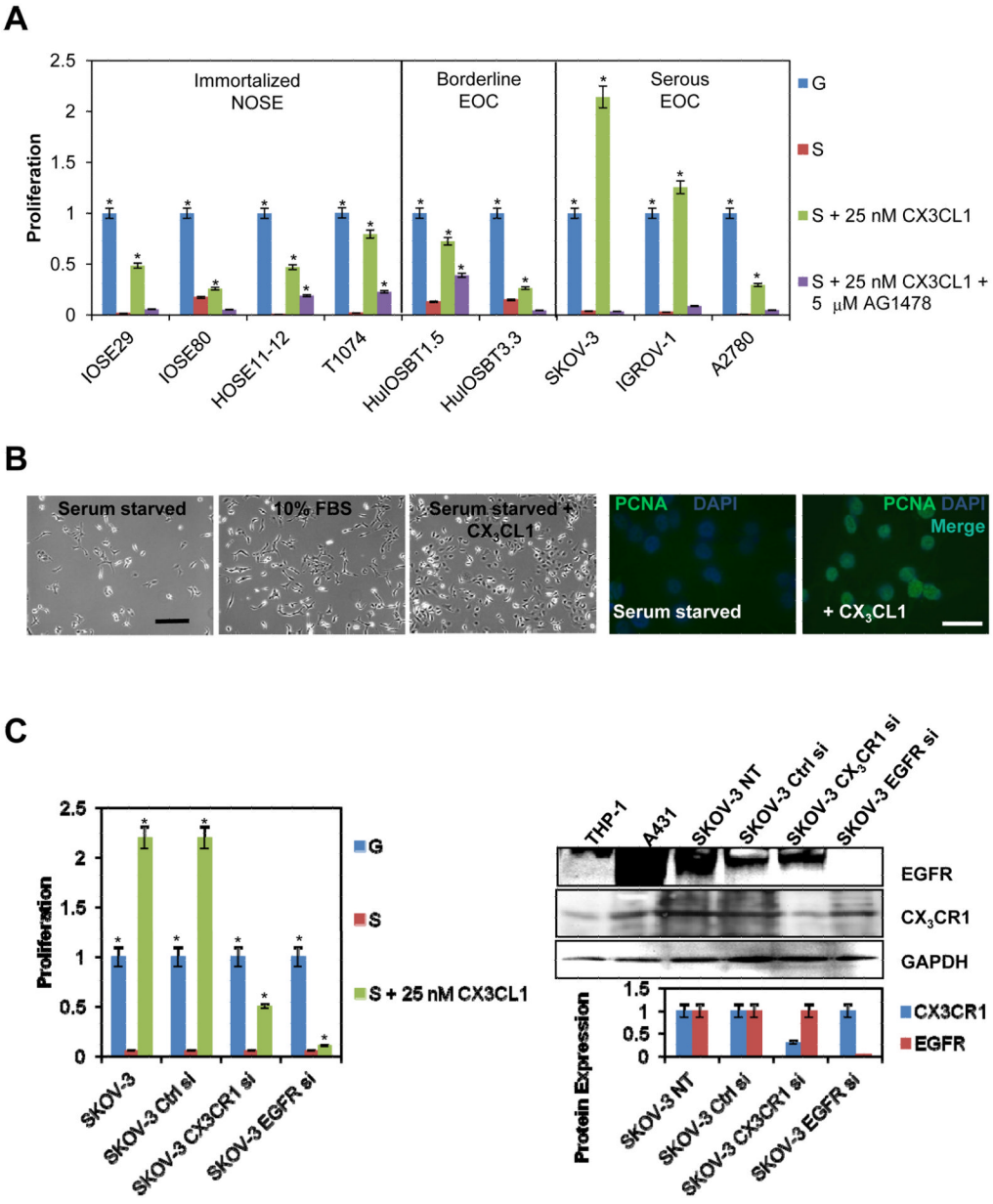

Figure 6. CX_3CL1 is instrumental in promoting cell proliferation

(A) The proliferation rates of serum-starved IOSE, borderline EOC, and serous EOC cell lines were evaluated in the presence of 25 nM CX_3CL1 ("S + 25 nM CX_3CL1", green bars) or 25 nM CX_3CL1 plus 5 μM AG1478 ("S + 25 nM CX_3CL1 + 5μM AG1478", purple bars). Growth phase cells cultured in complete media containing 10% FBS were used as a positive control ("G", blue bars). Serum-starved cells were used as a negative control ("S", red bars). These data represent the average of three experiments performed in triplicate. *p<0.05. (B) SKOV-3 cells were serum-starved overnight, then one group was exposed to complete medium containing 10% FBS, second group was serum-starved, and the third group was treated with 25 nM CX_3CL1 in serum-free medium for 24 h, and photographed using a Zeiss microscope with a 5× objective. Bar, 100 μm. Nuclear PCNA staining (green) was evaluated by immunofluorescence. Nuclei were stained with DAPI (blue). Fluorescent images were generated using a Zeiss AxioObserver fluorescent microscope with a 40×

objective. Images were collected independently on the green and blue filters and subsequently superimposed. Bar, 20 μm. (C) SKOV-3 cells that were not transfected, transfected with control, CX_3CR1-specific, or EGFR-specific siRNAs were subjected to the cell proliferation assay in the presence of 25 nM CX_3CL1 ("S + 25 nM CX_3CL1 Growth phase cells cultured in complete media containing 10% FBS were used as a positive control ("G", blue bars). Serum-starved cells were used as a negative control ("S", red bars). Data represent the average of three experiments performed in triplicate. *$p<0.05$. Expression of CX_3CR1 and EGFR in transfected and non-transfected SKOV-3 cells was determined by Western blot. GAPDH served as a loading control. THP-1 and A431 cell lysates were used as positive controls for expression of CX_3CR1 and EGFR, respectively. Histograms demonstrate the levels of CX_3CR1 and EGFR expression, as determined by digital densitometry. *$p<0.05$.

Table 1

Concentration of CX_3CL1 in samples of ovarian carcinoma and borderline gynecologic diseases determined by ELISA.

Sample		CX_3CL1	
#	Diagnosis	ng/ml	nM
1	Borderline endometrioid cystadenoma	2.50	0.29
2	Borderline mucinous cystadenoma	0.86	0.10
3	Serous cyst	1.25	0.15
4	Serous adenocarcinoma, Stage IV, Grade 3	20.00	2.30
5	Serous adenocarcinoma, Stage IV	25.00	3.00
6	Serous adenocarcinoma, Stage IIIc, Grade 3	25.00	3.00